Local discretization method for overdamped Brownian motion on a potential with multiple deep wells

P. T. T. Nguyen
Scion, Private Bag 3020, Rotorua 3046, New Zealand
and Department of Physics, University of Otago, P. O. Box 56, Dunedin 9054, New Zealand

K. J. Challis
Scion, Private Bag 3020, Rotorua 3046, New Zealand

M. W. Jack*
Department of Physics, University of Otago, P. O. Box 56, Dunedin 9054, New Zealand
(Received 24 August 2016; published 17 November 2016)

We present a general method for transforming the continuous diffusion equation describing overdamped Brownian motion on a time-independent potential with multiple deep wells to a discrete master equation. The method is based on an expansion in localized basis states of local metastable potentials that match the full potential in the region of each potential well. Unlike previous basis methods for discretizing Brownian motion on a potential, this approach is valid for periodic potentials with varying multiple deep wells per period and can also be applied to nonperiodic systems. We apply the method to a range of potentials and find that potential wells that are deep compared to five times the thermal energy can be associated with a discrete localized state while shallower wells are better incorporated into the local metastable potentials of neighboring deep potential wells.

DOI: 10.1103/PhysRevE.94.052127

I. INTRODUCTION

Brownian motion on a potential has been used to describe many nonequilibrium systems with thermal fluctuations, including electrical circuits (Josephson effect) [1–3], colloidal condensed matter systems such as supercooled liquids and soft materials [4], ion channels [5–7], and molecular motors [8–11]. When the potential is characterized by multiple deep wells, it is physically intuitive that the continuous diffusion equation for the system can be approximated by a simpler discrete master equation describing infrequent hopping transitions between wells. In this paper, we develop a discretization method that expands the continuous diffusion equation on a localized basis of states to formally derive a discrete master equation. This approach can be applied to a wide range of time-independent potentials with multiple deep wells.

The standard theoretical description of overdamped Brownian motion on a time-independent potential is via a continuous diffusion equation that governs the probability density $P(x,t)$ at position x and time t [8,9]:

$$\frac{\partial P(x,t)}{\partial t} = \mathcal{L}P(x,t), \tag{1}$$

$$\mathcal{L} = \frac{1}{\gamma}\frac{\partial}{\partial x}\left[\Theta\frac{\partial}{\partial x} + \frac{\partial V(x)}{\partial x}\right], \tag{2}$$

where $\mathcal{L}$ is the evolution operator, $V(x)$ is the potential, $\Theta = k_B T$, k_B is the Boltzmann constant, T is the temperature, and γ is the friction coefficient. In the limit of deep potential wells, the continuous diffusion equation can be approximated by a discrete master equation describing infrequent hopping between adjacent wells:

$$\frac{dp_n(t)}{dt} = \kappa_{n,n-1}p_{n-1}(t) + \kappa_{n,n+1}p_{n+1}(t) - (\kappa_{n+1,n} + \kappa_{n-1,n})p_n(t), \tag{3}$$

where p_n is the probability of the system being confined in the nth well of the potential $V(x)$ and $\kappa_{n,n'}$ (with $|n-n'|=1$) is the rate of hopping between neighboring wells. The master equation is significantly simpler than the original continuous diffusion equation and can be used to calculate measurable properties of the system such as the drift velocity and diffusion [12], kinetics [13], dwell time statistics [14–17], and (in the context of molecular motors) energy coupling [18–21].

Attempts to transform the continuous diffusion equation (1) to a discrete master equation (3) have had varying levels of mathematical rigor and applicability. It has been suggested that the master equation can be made consistent with the diffusion equation by matching system properties such as the dynamic structure factor [22–24], the eigenvalues [25], or the ratio between forward and backward hopping [26]. Alternatively, a master equation can be written to describe hopping between nearest-neighbor spatial cells and the hopping rates calculated using local steady-state solutions [27,28]. Yet another approach, interpreting the master equation in terms of hopping between neighboring deep potential wells, determines the hopping rates using first passage times or splitting probabilities [6,29,30]. In contrast, we use the classical analog of the tight-binding method where we expand on a localized basis of states to transform the continuous diffusion equation to a discrete master equation. This method formally connects the hopping rates $\kappa_{n,n'}$ of the master equation to the potential and allows the regime of validity of the master equation to be determined explicitly.

*michael.jack@otago.ac.nz

The tight-binding method was originally developed for the quantum system of an electron in a solid [31]. In that case, the continuous Schrödinger equation describing the system evolution is systematically transformed to a discrete equation by expanding in a basis of localized states. There are two approaches to deriving the tight-binding model. One approach exploits the periodicity of the potential by using localized Wannier states formulated in terms of Bloch eigenfunctions of the system [32–36]. The other approach uses atomic orbitals of an isolated atom as a set of basis states for the electron [31,37]. In previous work, we developed the Brownian-motion analog of the Wannier-state method [21,38,39]. This works well for periodic potentials with a single dominant minimum per period [21,38] or for bichromatic periodic potentials with multiple similar wells per period [39]. However, the Wannier-state approach is not suitable for nonperiodic potentials or periodic potentials with varying multiple deep wells per period. In this paper, we develop a Brownian-motion analog of the atomic-orbital tight-binding method that can be used to derive a discrete master equation for general potentials with multiple deep wells.

To develop an atomic-orbital tight-binding method for Brownian motion on a potential, we expand the continuous evolution equation in localized eigenfunctions of local potentials defined around each deep potential well. The local potential for each well matches the full potential in the region of that well. When defining the local potentials and basis states, we consider the following. First, unlike the quantum case, the evolution operator for Brownian motion on a potential is not self-adjoint. Therefore, a biorthonormal basis must be constructed using not only the eigenfunctions $\psi_k(x)$ of the evolution operator $\mathcal{L}$, i.e., $\mathcal{L}\psi_k(x) = -\nu_k\psi_k(x)$ with eigenvalues ν_k, but also the adjoint eigenfunctions $\psi_k^\dagger(x)$ of the adjoint operator

$$\mathcal{L}^\dagger = \frac{1}{\gamma}\left[\Theta\frac{\partial^2}{\partial x^2} - \frac{\partial V(x)}{\partial x}\frac{\partial}{\partial x}\right], \tag{4}$$

i.e., $\mathcal{L}^\dagger\psi_k^\dagger(x) = -\nu_k^\dagger\psi_k^\dagger(x)$ with adjoint eigenvalues $\nu_k^\dagger = \nu_k$ [8]. Second, choosing *confining* local potentials around each potential well, i.e., taking the local potentials to positive infinity at their boundaries, would mean that the ground-state eigenvalue is zero ($\nu_1 = \nu_1^\dagger = 0$) and while the eigenfunctions $\psi_k(x)$ would be localized, the ground adjoint eigenfunctions $\psi_1^\dagger(x) = 1$ would not be localized [8]. Both the eigenfunctions and their adjoints must be localized in order to assign probability to a particular well (see Sec. III). Therefore, to construct a fully localized biorthonormal basis, we define local *metastable* potentials around each potential well. Each local metastable potential matches the full potential in the region around its minimum, including both adjacent maxima, and goes to minus infinity at its boundaries. This approach ensures the localization of the basis states and their adjoints. By expanding in the eigenfunctions of local metastable potentials, we systematically derive a discrete master equation for Brownian motion on a potential with multiple deep potential wells. We evaluate the applicability of the method numerically for a range of different potentials.

This paper is organized as follows. In Sec. II we construct a localized basis for Brownian motion on a time-independent potential with multiple deep potential wells using eigenfunctions of local metastable potentials. In Sec. III we expand the probability density on the localized basis and transform the continuous evolution equation to a discrete master equation. In Sec. IV we apply the method to particular periodic and nonperiodic potentials. We conclude in Sec. V.

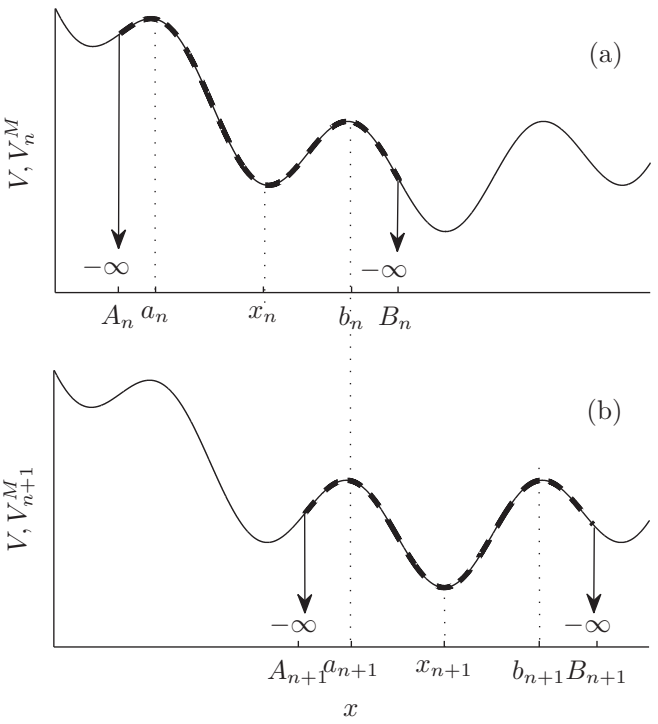

FIG. 1. A potential with multiple wells (solid) showing the local metastable potentials defined by Eq. (5) (dashed) for the nth (a) and $(n+1)$th (b) potential wells.

II. LOCALIZED BASIS

We consider the continuous diffusion equations (1) and (2) with a time-independent potential characterized by multiple deep wells, as shown in Fig. 1. For each potential well n, we define a local metastable potential $V_n^M(x)$ with a minimum at $x = x_n$ and adjacent maxima at $x = a_n$ and $x = b_n$. Each metastable potential is defined in terms of the full system potential $V(x)$ as

$$V_n^M(x) = \begin{cases} V(x) & A_n < x < B_n \\ -\infty & x = A_n, \quad x = B_n \end{cases}, \tag{5}$$

where the boundaries A_n and B_n of the potential are chosen arbitrarily with $x_{n-1} \leqslant A_n < a_n$ and $b_n < B_n \leqslant x_{n+1}$. The metastable potentials $V_n^M(x)$ and $V_{n+1}^M(x)$ overlap in the interval $A_{n+1} < x < B_n$ around the common maximum $b_n = a_{n+1}$.

The eigenfunction expansion of overdamped Brownian motion on a metastable potential is well known [8]. Briefly, the eigenfunctions $\psi_{n,m}(x)$ and adjoints $\psi_{n,m}^\dagger(x)$ of the nth metastable potential are given by

$$\mathcal{L}_n^M\psi_{n,m}(x) = -\nu_{n,m}\psi_{n,m}(x), \tag{6}$$

$$\mathcal{L}_n^{M\dagger}\psi_{n,m}^\dagger(x) = -\nu_{n,m}\psi_{n,m}^\dagger(x), \tag{7}$$

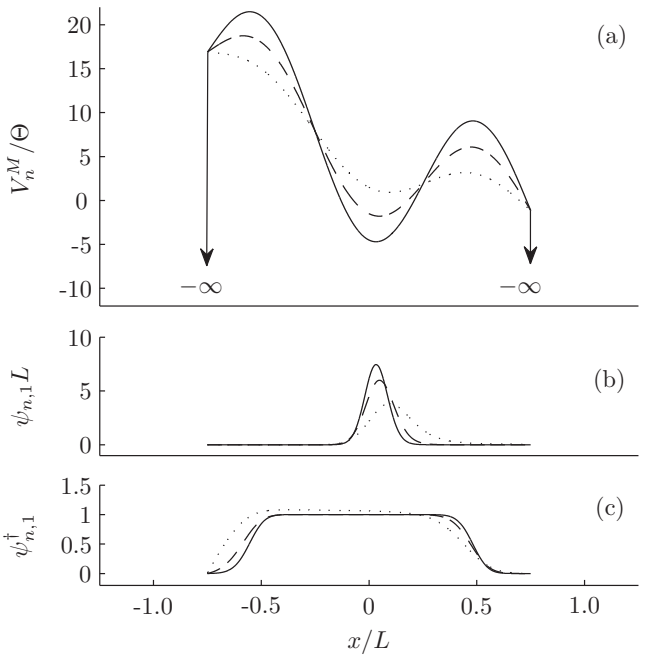

FIG. 2. A metastable potential with differing barrier heights high (solid), mid (dash), and low (dot) (a). The ground eigenfunction (b) and the ground adjoint function (c) for the metastable potential in (a).

where $\mathcal{L}_n^M$ and $\mathcal{L}_n^{M\dagger}$ are, respectively, the evolution operator and its adjoint for the metastable potential $V_n^M(x)$ on the nth well. In Eqs. (6) and (7), $\nu_{n,m}$ are the eigenvalues of the nth metastable potential and $m \geqslant 1$ labels the eigenvalues in that potential (with increasing magnitude). For a given n, the eigenfunctions $\psi_{n,m}(x)$ and adjoints $\psi_{n,m}^\dagger(x)$ form a complete biorthogonal set on the interval $A_n \leqslant x \leqslant B_n$ [8], i.e.,

$$\sum_m \psi_{n,m}^\dagger(y)\psi_{n,m}(x) = \delta(x-y), \tag{8}$$

for $A_n \leqslant x \leqslant B_n$ and $A_n \leqslant y \leqslant B_n$. It is convenient to normalize the eigenfunctions by

$$\int_{A_n}^{B_n} dx\ \psi_{n,m'}^\dagger(x)\psi_{n,m}(x) = \delta_{mm'}, \tag{9}$$

and we normalize the ground ($m = 1$) eigenfunctions such that

$$\int_{A_n}^{B_n} dx\ \psi_{n,1}(x) = 1. \tag{10}$$

Figure 2 shows the form of $\psi_{n,1}(x)$ and $\psi_{n,1}^\dagger(x)$ for a metastable potential with characteristic length L and a range of potential barrier heights. Both the ground eigenfunctions and their adjoints are localized for potentials that are deep compared to the thermal energy Θ. As the potential minimum becomes deeper, the eigenfunctions $\psi_{n,1}(x)$ become more localized and the adjoints $\psi_{n,1}^\dagger(x)$ become closer to unity at the potential minimum $x = x_n$. Approximate analytical forms of $\psi_{n,1}(x)$ and $\psi_{n,1}^\dagger(x)$ are given in Appendix A. In the limit of an infinitely deep metastable potential, the eigenfunctions and their adjoints coincide with the eigenfunctions and adjoints of the confined system that matches the metastable potential in the region of the deep well.

The probability density $P_n^M(x,t)$ for the metastable potential $V_n^M(x)$ can be expanded in the complete biorthonormal basis of eigenfunctions as

$$P_n^M(x,t) = \sum_m c_{n,m}(t)\psi_{n,m}(x), \tag{11}$$

where the expansion coefficients

$$c_{n,m}(t) = \int_{A_n}^{B_n} dx\ \psi_{n,m}^\dagger(x)P_n^M(x,t), \tag{12}$$

decay in time according to

$$c_{n,m}(t) = c_{n,m}(0)e^{-\nu_{n,m}t}. \tag{13}$$

The probability current for the nth metastable potential is

$$J_n^M(x,t) = \mathcal{J}_n^M P_n^M(x,t), \tag{14}$$

$$\mathcal{J}_n^M = -\frac{1}{\gamma}\left[\Theta\frac{\partial}{\partial x} + \frac{\partial V_n^M(x)}{\partial x}\right], \tag{15}$$

where $\mathcal{J}_n^M$ is the current operator for the nth metastable potential and the evolution and current operators are related by

$$\mathcal{L}_n^M = -\frac{\partial}{\partial x}\mathcal{J}_n^M. \tag{16}$$

Inserting the expansion Eq. (11), the probability current Eq. (14) can be written as

$$J_n^M(x,t) = \sum_m c_{n,m}(t)J_{n,m}(x), \tag{17}$$

where the probability current for the mth eigenfunction of the nth metastable potential is

$$J_{n,m}(x) = \mathcal{J}_n^M\psi_{n,m}(x). \tag{18}$$

By definition, the probability current $J_{n,m}(x)$ does not vanish at the boundaries A_n and B_n and this is important in the transformation of the continuous diffusion equation to a discrete master equation in Sec. III. Using the eigenequation Eq. (6), with Eqs. (16) and (18), we find that

$$\frac{\partial}{\partial x}J_{n,m}(x) = \nu_{n,m}\psi_{n,m}(x). \tag{19}$$

Integrating Eq. (19) from A_n to B_n, we derive for the ground ($m = 1$) state

$$J_{n,1}(B_n) - J_{n,1}(A_n) = \nu_{n,1}, \tag{20}$$

where we have used the normalization Eq. (10). Physically, Eq. (20) states that the decay rate of the ground eigenfunction of a metastable potential equals the sum of the outward eigenfunction current at the boundary of the metastable potential. In the deep well regime, the boundary currents $J_{n,1}(A_n)$ and $J_{n,1}(B_n)$ are well approximated by Kramers' escape rate over the left and right potential maxima, respectively, as shown in Appendix A, and the lowest eigenvalue $\nu_{n,1}$ is related to the inverse mean escape time from the metastable potential [8].

We define localized states of the full system in terms of the eigenfunctions of the local metastable potentials as follows:

$$\omega_{n,m}(x) = \begin{cases} \psi_{n,m}(x) & A_n \leqslant x \leqslant B_n \\ 0 & x < A_n, x > B_n \end{cases}, \tag{21}$$

$$\omega^\dagger_{n,m}(x) = \begin{cases} \psi^\dagger_{n,m}(x) & A_n \leqslant x \leqslant B_n \\ 0 & x < A_n, \quad x > B_n \end{cases}. \tag{22}$$

The localized states $\omega_{n,m}(x)$ and $\omega^\dagger_{n,m}(x)$ are continuous and for each n form a biorthonormal set, i.e.,

$$\int_{-\infty}^{\infty} dx\ \omega^\dagger_{n,m'}(x)\omega_{n,m}(x) = \delta_{mm'}. \tag{23}$$

The ground eigenfunctions $\psi_{n,1}(x)$ satisfy the normalization Eq. (10) so the ground localized states satisfy

$$\int_{-\infty}^{\infty} dx\ \omega_{n,1}(x) = 1. \tag{24}$$

The states $\omega_{n,m}(x)$ and $\omega^\dagger_{n,m}(x)$ also form a complete set on the interval $A_n \leqslant x \leqslant B_n$ due to the completeness relation Eq. (8). Therefore, the full state basis, including $\omega_{n,m}(x)$ and $\omega^\dagger_{n,m}(x)$ for all n and m, is complete for the full system and is overcomplete in the overlapping intervals $A_{n+1} \leqslant x \leqslant B_n$. Formally,

$$\sum_{n,m} \omega_{n,m}(y)\omega^\dagger_{n,m}(x) = \delta(x-y), \tag{25}$$

for any x and y.

The probability current for the state $\omega_{n,m}(x)$ is

$$J^\omega_{n,m}(x) = \mathcal{J}\omega_{n,m}(x), \tag{26}$$

where the current operator is

$$\mathcal{J} = -\frac{1}{\gamma}\left[\Theta\frac{\partial}{\partial x} + \frac{\partial V(x)}{\partial x}\right]. \tag{27}$$

The probability current can be written piecewise as

$$J^\omega_{n,m}(x) = \begin{cases} J_{n,m}(x) & A_n < x < B_n \\ 0 & x < A_n, \quad x > B_n \end{cases}. \tag{28}$$

Due to the absorbing boundary conditions, $J^\omega_{n,m}(x)$ is discontinuous at the boundaries A_n and B_n, as shown in Fig. 3. The limits can be taken at the boundary as follows:

$$\lim_{x\to A_n^-} J^\omega_{n,m}(x) = 0, \quad \lim_{x\to A_n^+} J^\omega_{n,m}(x) = J_{n,m}(A_n), \tag{29}$$

$$\lim_{x\to B_n^+} J^\omega_{n,m}(x) = 0, \quad \lim_{x\to B_n^-} J^\omega_{n,m}(x) = J_{n,m}(B_n), \tag{30}$$

where $J_{n,m}(A_n)$ and $J_{n,m}(B_n)$ are the boundary probability currents for the eigenfunctions of the nth metastable potential.

III. DISCRETE MASTER EQUATION

The localized states $\omega_{n,m}(x)$ and $\omega^\dagger_{n,m}(x)$ defined in Sec. II form a complete basis. Therefore, we expand the probability density of the full system as

$$P(x,t) = \sum_{n',m'} p_{n',m'}(t)\omega_{n',m'}(x), \tag{31}$$

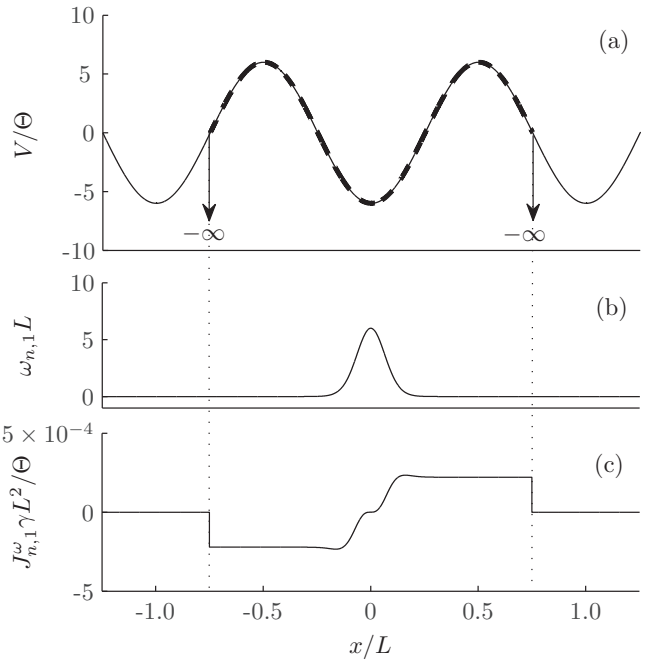

FIG. 3. A potential with multiple wells (solid) showing a symmetric metastable potential (dashed) (a). The ground localized state (b) for the metastable potential in (a) and the current (c) for the state in (b).

where

$$p_{n,m}(t) = \int dx\ \omega^\dagger_{n,m}(x)P(x,t). \tag{32}$$

Inserting expansion Eq. (31) into the evolution equation (1), multiplying to the left by $\omega^\dagger_{n,m}(x)$ and integrating, we transform the evolution equation to

$$\sum_{n',m'} M_{n,n',m,m'}\frac{dp_{n',m'}(t)}{dt} = \sum_{n',m'} \sigma_{n,n',m,m'}\,p_{n',m'}(t), \tag{33}$$

where the biorthonormality and overcompleteness of the states is measured by the *overlap matrix*

$$M_{n,n',m,m'} = \int dx\ \omega^\dagger_{n,m}(x)\omega_{n',m'}(x), \tag{34}$$

and the *coupling constant* is

$$\sigma_{n,n',m,m'} = \int dx\ \omega^\dagger_{n,m}(x)\mathcal{L}\omega_{n',m'}(x). \tag{35}$$

We evaluate the coupling constant as follows. The state $\omega_{n',m'}(x)$ vanishes outside the boundaries $A_{n'}$ and $B_{n'}$ and $\mathcal{L}\omega_{n',m'}(x)$ is discontinuous at these boundaries. Therefore, the coupling constant can be written as

$$\begin{aligned}\sigma_{n,n',m,m'} = \lim_{\Delta x\to 0}\Bigg\{&\int_{A_{n'}+\Delta x}^{B_{n'}-\Delta x} dx\ \omega^\dagger_{n,m}(x)\mathcal{L}\omega_{n',m'}(x) \\ &+ \int_{A_{n'}-\Delta x}^{A_{n'}+\Delta x} dx\ \omega^\dagger_{n,m}(x)\mathcal{L}\omega_{n',m'}(x) \\ &+ \int_{B_{n'}-\Delta x}^{B_{n'}+\Delta x} dx\ \omega^\dagger_{n,m}(x)\mathcal{L}\omega_{n',m'}(x)\Bigg\}.\end{aligned} \tag{36}$$

In the first term on the right-hand side of Eq. (36), we use the replacement $\mathcal{L}\omega_{n',m'}(x) = -\nu_{n',m'}\omega_{n',m'}(x)$. In the second and third terms we use the chain rule and the current properties Eqs. (29) and (30). This gives

$$\begin{aligned}\sigma_{n,n',m,m'} &= -\nu_{n',m'}M_{n,n',m,m'} \\ &+\omega^{\dagger}_{n,m}(B_{n'})J_{n',m'}(B_{n'}) - \omega^{\dagger}_{n,m}(A_{n'})J_{n',m'}(A_{n'}) \\ &+ \lim_{\Delta x\to 0}\left\{\int_{A_{n'}-\Delta x}^{A_{n'}+\Delta x} dx\; J^{\omega}_{n',m'}(x)\frac{d\omega^{\dagger}_{n,m}(x)}{dx}\right. \\ &\left.+\int_{B_{n'}-\Delta x}^{B_{n'}+\Delta x} dx\; J^{\omega}_{n',m'}(x)\frac{d\omega^{\dagger}_{n,m}(x)}{dx}\right\}. \qquad (37)\end{aligned}$$

Taking $n = n'$, the states $\omega_{n,m}(x)$ and $\omega^{\dagger}_{n,m'}(x)$ are biorthonormal by Eq. (23), $\omega^{\dagger}_{n,m}(B_n) = \omega^{\dagger}_{n,m}(A_n) = 0$ due to the absorbing boundary condition for the metastable potentials, and $d\omega^{\dagger}_{n,m}(A_n)/dx \approx d\omega^{\dagger}_{n,m}(B_n)/dx \approx 0$. Therefore, $M_{n,n,m,m'} = \delta_{mm'}$ and $\sigma_{n,n,m,m'} = -\nu_{n,m}\delta_{mm'}$. For $n \neq n'$, only adjacent regions overlap so, when $|n-n'| \geqslant 2$, $M_{n,n',m,m'} = 0$ and $\sigma_{n,n',m,m'} = 0$. Therefore, $\omega_{n,m}(x)$ only couples with itself and states in nearest-neighbor wells. Using these properties of the coupling constant and the overlap matrix, Eq. (33) simplifies to

$$\begin{aligned}\frac{dp_{n,m}(t)}{dt} &= -\nu_{n,m}\,p_{n,m}(t) + \sum_{n'=n\pm1,m'}\sigma_{n,n',m,m'}\,p_{n',m'}(t) \\ &- \sum_{n'=n\pm1,m'}M_{n,n',m,m'}\frac{dp_{n',m'}(t)}{dt}. \qquad (38)\end{aligned}$$

In the deep-well regime, the interwell hopping rates are the same order as the decay rates of the ground states and there is a separation of time scales between the evolution of the ground states from the rest, i.e., $\nu_{n,m>1} \gg \nu_{n',1}$ for all n and n'. In this regime, the higher states can be adiabatically eliminated, as follows. We assume that the evolution of the higher states is dominated by the first term in Eq. (38) and that the higher states rapidly decay to their steady state $\tilde{p}_{n,m}(t)$. Setting $d\tilde{p}_{n,m>1}(t)/dt = 0$, we have for the higher states

$$\begin{aligned}\tilde{p}_{n,m>1}(t) &= \frac{1}{\nu_{n,m}}\sum_{n'=n\pm1}\sigma_{n,n',m,1}\,p_{n',1}(t) \\ &\frac{1}{\nu_{n,m}}\sum_{n'=n\pm1,m'>1}\sigma_{n,n',m,m'}\tilde{p}_{n',m'}(t) \\ &-\frac{1}{\nu_{n,m}}\sum_{n'=n\pm1}M_{n,n',m,1}\frac{dp_{n',1}(t)}{dt}, \qquad (39)\end{aligned}$$

and for the ground states

$$\begin{aligned}\frac{dp_{n,1}(t)}{dt} &= -\nu_{n,1}\,p_{n,1}(t) + \sum_{n'=n\pm1}\sigma_{n,n',1,1}\,p_{n',1}(t) \\ &+ \sum_{n'=n\pm1,m'>1}\sigma_{n,n',1,m'}\tilde{p}_{n',m'}(t) \\ &- \sum_{n'=n\pm1}M_{n,n',1,1}\frac{dp_{n',1}(t)}{dt}. \qquad (40)\end{aligned}$$

Substituting Eq. (39) for the higher states into Eq. (40) shows that the terms on the second-line of Eq. (40) are smaller than the other terms on the right-hand side and can be neglected to first order in $\epsilon = \nu_{n,1}/\nu_{n',m>1}$. This can be made rigorous via a perturbation treatment in the small parameter ϵ.

Two additional assumptions are required to unambiguously assign probability to individual potential wells and derive a consistent master equation. First, we assume that the ground states are localized to a single potential well and do not overlap. Formally, the ground states form a biorthonormal set (see Appendix A), i.e.,

$$M_{n,n',1,1} \approx \delta_{nn'}. \qquad (41)$$

Equation (40) can then be written in the form of a master equation for the lowest $m = 1$ band, i.e.,

$$\frac{dp_n(t)}{dt} = \sum_{n'=n,n\pm1}\kappa_{n,n'}\,p_{n'}(t), \qquad (42)$$

where we have dropped the $m = 1$ index in $p_{n,1}(t)$ and $\kappa_{n,n'} = \sigma_{n,n',1,1}$ is given by Eq. (37). Second, we assume that the ground adjoint states $\omega^{\dagger}_{n,1}(x)$ are localized to a single potential well and are approximately flat and equal to unity in that region. Formally, the ground adjoint states satisfy

$$\omega^{\dagger}_{n,1}(B_{n-1}) \approx 1, \quad \frac{d\omega^{\dagger}_{n,1}(B_{n-1})}{dx} \approx 0, \qquad (43)$$

$$\omega^{\dagger}_{n,1}(A_{n+1}) \approx 1, \quad \frac{d\omega^{\dagger}_{n,1}(A_{n+1})}{dx} \approx 0, \qquad (44)$$

so that the nth adjoint state is flat and equal to unity at the boundaries B_{n-1} and A_{n+1} of the adjacent metastable potentials (see Figs. 1 and 2). These boundaries B_{n-1} and A_{n+1} lie inside the maxima of the nth metastable potential. Equations (43) and (44) are satisfied in the deep well regime, as suggested by Fig. 2 and Appendix A. Using Eqs. (43) and (44) to evaluate the coupling constant Eq. (37) yields

$$\kappa_{n,n} = -\nu_{n,1}, \qquad (45)$$

$$\kappa_{n,n-1} = J_{n-1,1}(B_{n-1}), \qquad (46)$$

$$\kappa_{n,n+1} = -J_{n+1,1}(A_{n+1}). \qquad (47)$$

Using the current property Eq. (20), we find that

$$\sum_{n'=n,n\pm1}\kappa_{n',n} = -\nu_{n,1} + J_{n,1}(B_n) - J_{n,1}(A_n) = 0. \qquad (48)$$

The identity Eq. (48) ensures that the master equation conserves probability, i.e., $\sum_n p_n(t)$ is constant, and allows the lowest-band master equation Eq. (42) to be written in the form of Eq. (3).

In summary, we have shown that the master equation Eq. (3) is a valid description of the system for time scales associated with the lowest band when (i) the decay rates of the higher states $\omega_{n,m>1}(x)$ are much larger than both the decay rates of the ground states $\omega_{n,1}(x)$ (i.e., $\nu_{n,1} \ll \nu_{n',m>1}$) and the rates of interwell hopping; (ii) the ground states $\omega_{n,1}(x)$ form a biorthonormal set; and (iii) the adjoint ground states satisfy Eqs. (43) and (44). All these conditions are satisfied in the limit of deep potential wells where $V(a_n) - V(x_n), V(b_n) - V(x_n) \gg \Theta$ for all n.

IV. APPLICATION

In this section, we numerically evaluate the applicability of the local discretization method for example periodic and nonperiodic potentials. First, we consider a regular periodic system where the potential wells have equal barrier height. Then we treat two systems where the potential wells have significantly different barrier heights. These latter cases cannot be treated by existing Wannier-state-based tight-binding approaches [21,38,39]. For each potential considered, we establish the validity of the discrete master equation by checking the three required assumptions: (i) we compare the decay rates of the higher states $\omega_{n,m>1}(x)$ with the decay rates of the ground states $\omega_{n,1}(x)$ by calculating the ratios $(\nu_{n,2}-\nu_{n,1})/\nu_{n,1}$; (ii) we check the biorthonormality of adjacent ground localized states by calculating

$$M_{n,n'} = \int dx\, \omega^{\dagger}_{n,1}(x)\omega_{n',1}(x), \tag{49}$$

and comparing it to the identity matrix using the Frobenius norm [40]; (iii) we compare the ground adjoint state $\omega^{\dagger}_{n,1}(x_n)$ at $x = x_n$ to unity and its derivative at $x = x_n$ to zero. In our calculations we choose the boundaries for the metastable states at $A_n = x_{n-1}$ and $B_n = x_{n+1}$.

To confirm that the master equation is a good approximation to the full continuous diffusion equation, we calculate the eigenvalues λ^{ME}_m of the master equation (42) and the eigenvalues λ^{FP}_m of the original evolution equation (1). To compare the eigenvalues, we calculate the ratios $\Delta_m = |\lambda^{FP}_m - \lambda^{ME}_m|/\lambda^{FP}_m$. For $m = 1$, $\lambda^{FP}_1 = 0$ so we take $\Delta_1 = |\lambda^{ME}_1 \gamma L^2/\Theta|$. We also calculate the probability density $P^{ME}(x,t) = \sum_n p_n(t)\omega_{n,1}(x)$ given by solving the master equation and the probability density $P^{FP}(x,t)$ determined by solving the original evolution equation (1) using an eigenfunction expansion. At each time point, the accuracy of the master equation can be measured by the integrated difference

$$\Delta P(t) = \int dx\, |P^{FP}(x,t) - P^{ME}(x,t)|. \tag{50}$$

At the steady state $t = t_{SS}$, we calculate the steady state probability density difference $\Delta P(t_{SS})$ where $P^{FP}(x,t_{SS})$ is the lowest eigenfunction of the continuous system and $P^{ME}(x,t_{SS})$ is calculated using the lowest eigenvector of the master equation.

A. Regular periodic system

We consider a three-well periodic potential of the form

$$V(x) = \frac{\mathcal{A}}{2}\cos(3qx), \tag{51}$$

where $q = 2\pi/L$ and we impose periodic boundary conditions at $x = 0$ and $x = L$. The three wells in each period have the same barrier height $|\mathcal{A}|$ and we define localized states for each potential well using the ground eigenfunctions of the metastable systems formed on each well (as described in Sec. II). The master equation for the three-well system has the form

$$\begin{aligned}
\frac{dp_1(t)}{dt} &= -(\kappa_{2,1}+\kappa_{3,1})p_1(t) + \kappa_{1,2}p_2(t) + \kappa_{1,3}p_3(t),\\
\frac{dp_2(t)}{dt} &= \kappa_{2,1}p_1(t) - (\kappa_{1,2}+\kappa_{3,2})p_2(t) + \kappa_{2,3}p_3(t),\\
\frac{dp_3(t)}{dt} &= \kappa_{3,1}p_1(t) + \kappa_{3,2}p_2(t) - (\kappa_{1,3}+\kappa_{2,3})p_3(t),
\end{aligned} \tag{52}$$

and has three eigenvalues λ^{ME}_m with $\lambda^{ME}_2 = \lambda^{ME}_3$. The hopping rates are in good agreement with Kramers' escape rate for deep wells (see Appendix B).

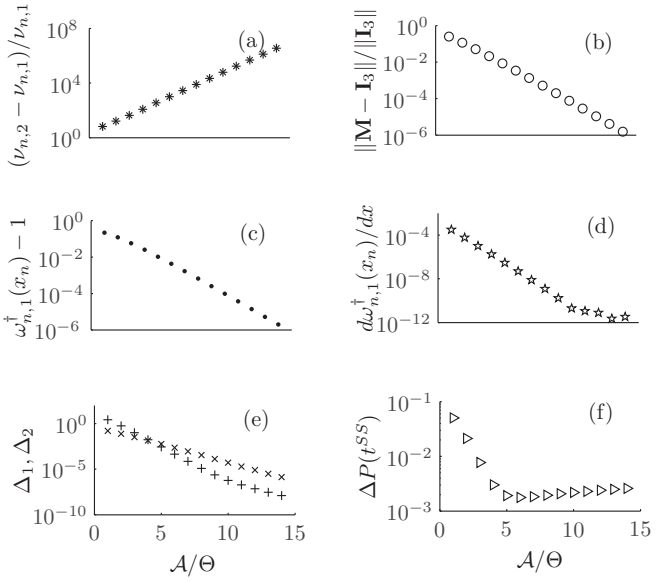

FIG. 4. The validity of master equation treatment Eq. (52) for the potential $V(x) = (\mathcal{A}/2)\cos(3qx)$ as a function of $\mathcal{A}$, as indicated by $(\nu_{n,2}-\nu_{n,1})/\nu_{n,1}$ (a), $\|\mathbf{M}-\mathbf{I}_3\|/\|\mathbf{I}_3\|$ (b), $\omega^{\dagger}_{n,1}(x_n)-1$ (c), $d\omega^{\dagger}_{n,1}(x_n)/dx$ (d), $\Delta_1 = |\lambda^{ME}_1\gamma L^2/\Theta|$ (plus), $\Delta_2 = |\lambda^{FP}_2 - \lambda^{ME}_2|/\lambda^{FP}_2$ (cross) (e), and $\Delta P(t^{SS}) = \int dx |P^{FP}(x,t^{SS}) - P^{ME}(x,t^{SS})|$ (f).

Figure 4 shows that increasing the barrier height $\mathcal{A}$ improves the validity of the master equation: (i) it increases the separation between the eigenvalues $\nu_{n,1}$ and $\nu_{n,2}$ for each metastable system, (ii) it improves the agreement between the matrix $\mathbf{M}$ of Eq. (49) and the identity matrix $\mathbf{I}$, and (iii) the ground adjoint state $\omega^{\dagger}_{n,1}(x)$ becomes closer to unity and its derivative becomes closer to zero at $x = x_n$. The exponential dependence of these metrics on barrier height is expected (see Appendix A).

For large $|\mathcal{A}|$, the eigenvalues of $\mathcal{L}$ separate into bands with the lowest band containing λ^{FP}_1, λ^{FP}_2, and λ^{FP}_3. Figure 4(e) shows that increasing the barrier height improves the agreement between the eigenvalues λ^{ME}_n derived from the master equation and the eigenvalues λ^{FP}_n derived from the original continuous equation. The ratio Δ_3 is not shown because $\lambda^{ME}_2 = \lambda^{ME}_3$ and $\lambda^{FP}_2 = \lambda^{FP}_3$. We also find that increasing the barrier height improves the agreement between the probability density calculated via the master equation and via the continuous equation. In particular, $\Delta P(t)$ decreases (increases) with time for large (small) values of $\mathcal{A}$. Figure 4(f)

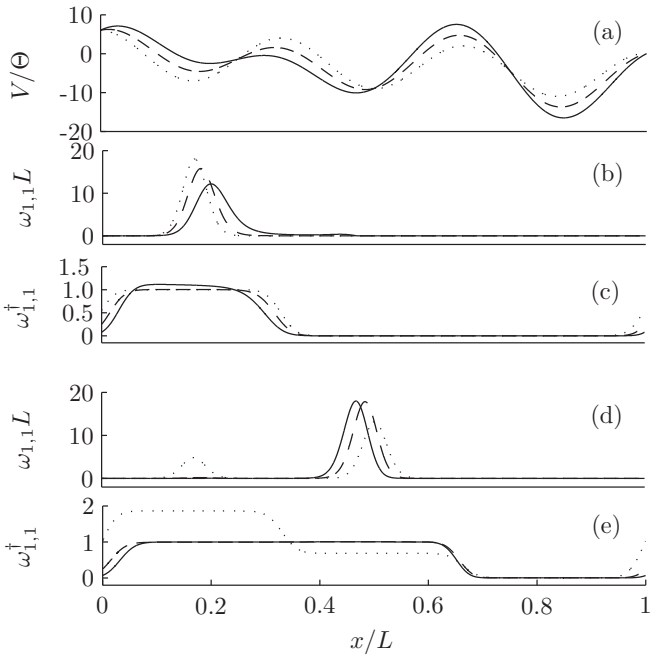

FIG. 5. Irregular three-well periodic potential Eq. (53) for $\mathcal{A}/\Theta = 12$, $\mathcal{F}L/\Theta = 6$, and $\mathcal{B}/\Theta = 0$ (dot), $\mathcal{B}/\Theta = 3$ (dash), and $\mathcal{B}/\Theta = 6$ (solid) (a). Localized state $\omega_{1,1}(x)$ (b) and adjoint state $\omega^\dagger_{1,1}(x)$ (c) for the first potential well. Combined localized state of the first and second potential wells (d) and associated adjoint state (e).

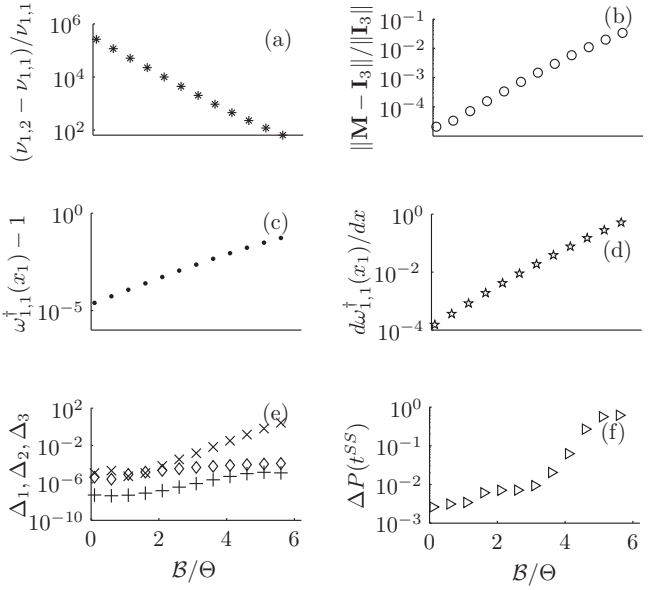

FIG. 6. The validity of three-state master equation treatment Eq. (52) for the potential Eq. (53) with $\mathcal{A}/\Theta = 12$ and $\mathcal{F}L/\Theta = 6$ as a function of $\mathcal{B}$, as indicated by $(\nu_{1,2}-\nu_{1,1})/\nu_{1,1}$ (a), $\|\mathbf{M}-\mathbf{I}_3\|/\|\mathbf{I}_3\|$ (b), $\omega^\dagger_{1,1}(x_1)-1$ (c), $d\omega^\dagger_{1,1}(x_1)/dx$ (d), Δ_1 (plus), Δ_2 (cross), Δ_3 (dimon) (e), and $\Delta P(t^{SS})$ (f).

shows the integrated probability function difference $\Delta P(t_{SS})$ at the steady state for varying $\mathcal{A}$.

As expected, we find that the master equation is valid for long times and deep wells. In particular, based on a threshold of a 1% difference between the eigenvalues of the master equation and the continuous equation, we find that the master equation provides a good description of the long-time dynamics of the system for $\mathcal{A}/\Theta \geqslant 5$.

B. Irregular periodic systems

For irregular periodic potentials that have wells with different depths, the appropriate master equation depends on the number of *deep* wells. To illustrate, we consider the three-well periodic potential

$$V(x) = \frac{\mathcal{A}}{2}\cos(3qx) + \mathcal{B}\sin(2qx) - \mathcal{F}x. \tag{53}$$

Figure 5(a) shows the irregular three-well potential Eq. (53) for different values of $\mathcal{B}$. In each case, the potential has three wells per period. However, as $\mathcal{B}$ increases the barrier between the first and second potential wells decreases while the barrier between the second and third potential wells increases. This means that for small $\mathcal{B}$, defining a localized state for each of the three potential wells yields a valid master equation. However, for large values of $\mathcal{B}$, the system is better approximated by a two-well system where the first two wells are combined to define one localized state and the third well defines the other. We establish the validity of these two alternative master equation treatments, as follows.

First, we consider a localized basis with three states, i.e., we define a localized $\omega_{n,1}(x)$ state for each of the three potential wells. This results in a master equation of the form of Eq. (52). As $\mathcal{B}$ increases the localized state $\omega_{1,1}(x)$ becomes broader and the adjoint state $\omega^\dagger_{1,1}(x_1)$ becomes increasingly different from unity with an increasing derivative, as shown in Figs. 5(b) and 5(c), respectively. Figure 6 shows that increasing $\mathcal{B}$ adversely affects all the assumptions required for the validity of the master equation, reduces the agreement between the eigenvalues of the master equation and those of the original evolution equation, and reduces the agreement between the steady-state probability density given by the master equation and by the original equation. For $\mathcal{B} \leqslant 3.5$ the first potential well (i.e., the shallowest well) is deeper than 5Θ, the difference between the eigenvalues of the master equation and the original equation is less than 1%, and the three-state master equation is valid for describing the system dynamics for long times. This indicates that when a potential well is deeper than approximately 5Θ, it can be treated as a localized state in a discrete master equation.

Second, we consider a localized basis with two states, i.e., we define one localized state that encompasses both the first and second potential wells and a second localized state for the third well. The local potential for the first two wells is a metastable potential that covers both the first and second potential wells and adjacent maxima. The localized state and its adjoint for the first and second wells is shown in Figs. 5(d) and 5(e). The master equation derived from the localized basis with two states has the form

$$\begin{aligned}\frac{dp_1(t)}{dt} &= -\kappa_{2,1}p_1(t) + \kappa_{1,2}p_2(t),\\ \frac{dp_2(t)}{dt} &= \kappa_{2,1}p_1(t) - \kappa_{1,2}p_2(t),\end{aligned} \tag{54}$$

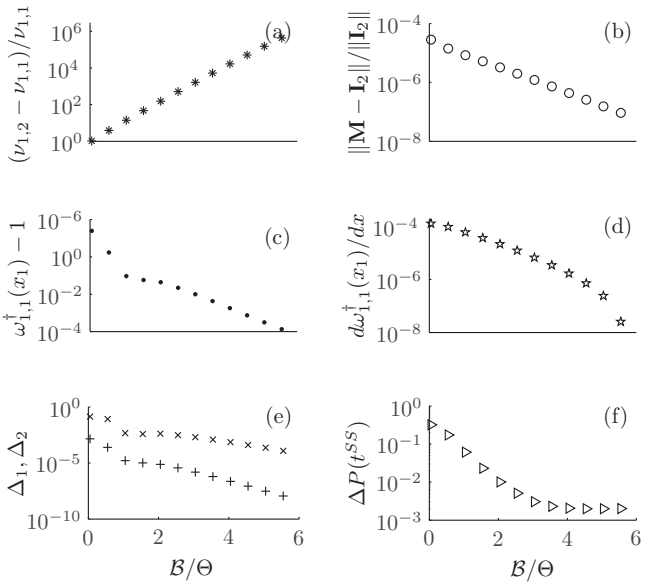

FIG. 7. The validity of the two-state master equation treatment Eq. (54) for the potential Eq. (53) with $\mathcal{A}/\Theta = 12$ and $\mathcal{F}L/\Theta = 6$ as a function of $\mathcal{B}$, as indicated by $(\nu_{1,2}-\nu_{1,1})/\nu_{1,1}$ (a), $\|\mathbf{M}-\mathbf{I}_2\|/\|\mathbf{I}_2\|$ (b), $|\omega^{\dagger}_{1,1}(x_1)-1|$ (c), $d\omega^{\dagger}_{1,1}(x_1)/dx$ (d), Δ_1 (plus), Δ_2 (cross) (e), and $\Delta P(t^{SS})$ (f).

and has two eigenvalues λ_1^{ME} and λ_2^{ME}. For $\mathcal{B} = 0$, we find that the ground state for the combined well has a clear two-peak structure and the adjoint state is not well approximated by unity across the combined well. However, increasing $\mathcal{B}$ decreases the barrier height between the first and second wells and increases the barrier heights of both the combined metastable potential for the first and second wells and the metastable potential for the third well. As shown in Fig. 7, increasing $\mathcal{B}$ improves all the assumptions required for the validity of the two-state master equation (54). Therefore, increasing $\mathcal{B}$ improves the agreement between the eigenvalues of the master equation and the lowest two eigenvalues of the original equation and improves the agreement between the steady-state probability density given by the master equation and by the original equation. Unlike the three-state master equation Eq. (52), the two-state master equation Eq. (54) does not capture the third eigenvalue λ_3^{FP}.

In summary, for the irregular three-well potential Eq. (53), the appropriate master equation depends on the number of deep wells. For small $\mathcal{B}$, all three wells of the potential are deep and have their own localized states. However, for large $\mathcal{B}$, the $n = 1$ well becomes too shallow to be described by its own localized state and is better incorporated into a combined well encompassing the first and second potential wells. The number of localized states involved in the long-time evolution of the system is indicated by the eigenvalue spectrum of the original evolution equation. We find that, for small $\mathcal{B}$, the lowest three eigenvalues λ_1^{FP}, λ_2^{FP}, and λ_3^{FP} are well separated from all the higher eigenvalues $\lambda_{m>3}^{FP}$ of the system. However, for large $\mathcal{B}$, the lowest two eigenvalues λ_1^{FP} and λ_2^{FP} are comparatively close while the eigenvalue λ_3^{FP} is closer to the higher eigenvalues $\lambda_{m>3}^{FP}$ than the lower two. This means that, for small $\mathcal{B}$, three states contribute to the long-time evolution of the system whereas, for large $\mathcal{B}$, the third eigenfunction has damped out leaving only two states contributing to the long-time evolution of the system. Based on a threshold of a 1% difference between the eigenvalues of the master equation and the continuous equation, we conclude that for $\mathcal{B} \leqslant 3.5$ the three-state master equation is valid while for $\mathcal{B} \geqslant 2$ the two-state master equation is valid. In the overlapping region $2 \leqslant \mathcal{B} \leqslant 3.5$, either approach can be used.

C. Nonperiodic system

The local discretization method can also be applied to nonperiodic potentials. For example, we consider the nonperiodic potential

$$V(x) = \frac{\mathcal{A}}{2}\cos(qx) + \mathcal{B}x^2, \tag{55}$$

where $q = 2\pi/L$ (L is periodicity of the periodic part). Due to the harmonic envelope function $\mathcal{B}x^2$, each potential well has asymmetric barrier heights and the difference between the two barrier heights increases with the distance from the origin at $x = 0$. For $9 \leqslant \mathcal{A}/\Theta \leqslant 12$ and $\mathcal{B}/\Theta = 6$, the potential has six wells with minima deep compared to 5Θ. We label these $1 \leqslant n \leqslant 6$ and define a localized state for each deep well. For $n = 1$ and $n = 6$, the metastable potentials are slightly altered from the usual definition to account for shallow potential wells up to the boundary. We write

$$V_1^M(x) = \begin{cases} \infty & x = -\tilde{A} \\ V(x) & -\tilde{A} < x < B_1 \\ -\infty & x = B_1 \end{cases}, \tag{56}$$

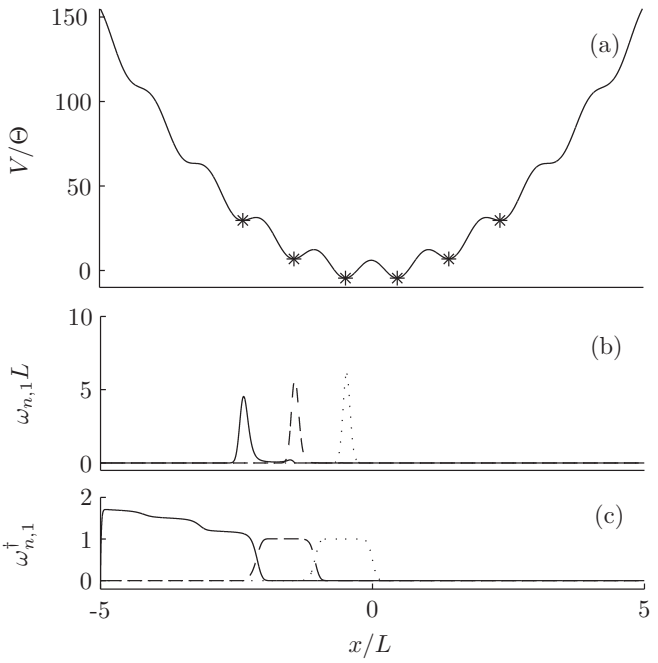

FIG. 8. Nonperiodic potential Eq. (55) for $\mathcal{A}/\Theta = 12$ and $\mathcal{B}/\Theta = 6$, $\tilde{A} = 5L$ (a). The stars indicate the potential minima of the six deep wells. States $\omega_{n,1}(x)$ (b) and adjoint states $\omega^{\dagger}_{n,1}(x)$ (c) for the wells $n = 1$ (solid), 2 (dash), and 3 (dot).

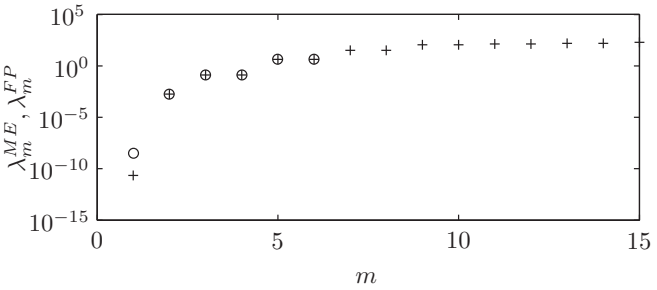

FIG. 9. Comparison of eigenvalues λ_m^{ME} of the master equation Eq. (58) (circle) and eigenvalues λ_m^{FP} of the original continuous equation (plus) for the potential in Fig. 8(a).

and

$$V_6^M(x) = \begin{cases} -\infty & x = A_6 \\ V(x) & A_6 < x < \tilde{A} \\ \infty & x = \tilde{A} \end{cases}. \tag{57}$$

The boundary at $x = -\tilde{A}$ and $x = \tilde{A}$ has been arbitrarily chosen sufficiently far from the origin to have no impact on the long-time evolution of the system. Figure 8 shows the potential Eq. (55) and the states $\omega_{n,1}(x)$ and their adjoints $\omega_{n,1}^{\dagger}(x)$ for $n = 1$, 2, and 3.

The master equation for the six localized states has the form

$$\frac{dp_n(t)}{dt} = \sum_{n'=n,n\pm1} \kappa_{n,n'} p_{n'}(t), \tag{58}$$

where $n = 1 - 6$, the sum is over nearest neighbors with $n = 1$ coupling only to $n = 2$ and $n = 6$ coupling only to $n = 5$. Equation (58) has six eigenvalues where $\lambda_3^{ME} = \lambda_4^{ME}$ and $\lambda_5^{ME} = \lambda_6^{ME}$. Figure 9 shows that the eigenvalues of the master equation are in good agreement with the six lowest eigenvalues of the original evolution equation. Unlike in the case of the irregular periodic potential of Sec. IV B, for the nonperiodic potential Eq. (55) there is no obvious gap in the eigenvalue spectrum of the original evolution equation (see Fig. 9). Therefore, the separation of time scales between the dynamics of the higher states and the dynamics of the lower states is not pronounced and the master equation is only valid when all the higher states have damped out.

V. CONCLUSION

We have derived a general discretization method for the continuous evolution equation for overdamped Brownian motion on a time-independent potential with multiple deep wells. This approach is based on an expansion in a set of localized basis states and is the Brownian-motion analog of the atomic orbital approach to the tight-binding model of quantum mechanics. For the Brownian motion case, the basis states are eigenfunctions of metastable potentials defined around each potential well. Expanding in these states provides a systematic derivation of a discrete master equation that is valid in the limit of deep potential wells.

The local discretization method is able to deal with a wide range of time-independent potentials with deep wells. A key advantage of the method is that it provides explicit measures for testing the validity of the derived discrete master equation. We have applied the local discretization method numerically for regular periodic, irregular periodic, and nonperiodic potentials. The results show that, for potentials with wells deeper than $5k_BT$, the long-time dynamics of the system is well approximated by a discrete master equation. For multiwell potentials with wells of significantly different depth, care should be taken when applying discretization approaches. In particular, potential wells shallower than $5k_BT$ should not be allocated their own localized state but rather are best treated by incorporating them into neighboring deep wells.

In the local discretization method, the rates of hopping between neighboring potential wells are derived formally. These hopping rates take into account the full details of the potential and, in the limit of deep wells, are consistent with alternative methods based on first passage times or splitting probabilities [6,29,30]. In particular, for deep wells, the ground localized states of the metastable potentials are in good agreement with the Boltzmann distribution and the hopping rates are given by the established Kramers' escape rate.

We have presented a one-dimensional treatment in this paper. However, in principle, the local discretization method can be extended to multidimensional cases. In more than one dimension, the metastable potentials have a closed boundary surface and key results such as Eq. (20) generalize to

$$\oint dS\, \mathbf{J}_{\mathbf{n},1}(\mathbf{x}) \cdot \hat{\mathbf{n}} = \nu_{n,1}, \tag{59}$$

where $\hat{\mathbf{n}}$ is the outward normal to the surface. Writing the left-hand side of Eq. (59) as a sum of discrete contributions would require localized current flow over saddle points and this suggests additional requirements for the application of a discrete master equation in multiple dimensions. The details of this are left for future work.

ACKNOWLEDGMENT

This work has been supported by Scion and by the Marsden Fund Council from Government funding, managed by the Royal Society of New Zealand.

APPENDIX A: ANALYTICAL APPROXIMATIONS TO THE METASTABLE EIGENFUNCTIONS AND RELATION TO KRAMERS' ESCAPE RATE

We consider a deep metastable potential $V(x)$ with minimum at x_n, neighboring adjacent maxima at a_n and b_n, and boundaries at A_n and B_n, as shown in Fig. 1. To first order in $\nu_{n,1}\gamma L^2/\Theta \ll 1$ (where $L \sim b_n - a_n$) the lowest eigenfunction and its adjoint can be approximated as [8]

$$\psi_{n,1}(x) = \mathcal{N} e^{-V(x)/\Theta} \psi_{n,1}^{\dagger}(x), \tag{A1}$$

$$\psi_{n,1}^{\dagger}(x) = 1 - \frac{I_n(x)}{I_n(B_n)} - \frac{\gamma \nu_{n,1}}{\Theta}\left[D_n(x) - \frac{I_n(x) D_n(B_n)}{I_n(B_n)}\right], \tag{A2}$$

where $A_n \leqslant x \leqslant B_n$,

$$\mathcal{N} = \int_{A_n}^{B_n} dy\, e^{-V(y)/\Theta}, \tag{A3}$$

$$\nu_{n,1} = \frac{1}{\gamma} \frac{I_n(B_n) - I_n(A_n)}{D_n(B_n) I_n(A_n) - D_n(A_n) I_n(B_n)}, \tag{A4}$$

and for notational convenience we define

$$I_n(x) = \int_{x_n}^{x} dy\, e^{V(y)/\Theta}, \tag{A5}$$

$$D_n(x) = \int_{x_n}^{x} dy \int_{x_n}^{y} dz\, e^{[V(y)-V(z)]/\Theta}. \tag{A6}$$

For deep potentials, the main contribution to $\psi_{n,1}(x)$ arises close to the minimum at $x = x_n$. Making a quadratic expansion about this point the dominant term is

$$\psi_{n,1}(x) \approx \sqrt{\frac{V''(x_n)}{2\pi\Theta}} e^{-V''(x_n)(x-x_n)^2/2\Theta}, \tag{A7}$$

where $V''(x)$ is the second derivative of the potential with respect to x. Similarly, the main contribution to the integrand of $I_n(x)$ arises close to the maxima of the potential. Making a quadratic expansion about the two maxima we have

$$\psi^{\dagger}_{n,1}(x) \approx \begin{cases} \frac{1}{2}\mathrm{erfc}[\sqrt{|V''(a_n)|/2\Theta}(a_n - x)], & A_n < x < x_n \\ \frac{1}{2}\mathrm{erfc}[\sqrt{|V''(b_n)|/2\Theta}(x - b_n)], & x_n > x > B_n \end{cases}, \tag{A8}$$

where erfc is the complementary error function and we have assumed that

$$\sqrt{|V''(a_n)|/2\Theta}(x_n - A_n) \gg 1, \tag{A9}$$

$$\sqrt{|V''(a_n)|/2\Theta}(x_n - a_n) \gg 1, \tag{A10}$$

$$\sqrt{|V''(b_n)|/2\Theta}(b_n - x_n) \gg 1, \tag{A11}$$

$$\sqrt{|V''(b_n)|/2\Theta}(B_n - x_n) \gg 1. \tag{A12}$$

For deep potential, the adjoint eigenfunction $\psi^{\dagger}_{n,1}(x)$ given by Eq. (A8) is equal to unity across the center of the metastable potential around x_n and then rapidly falls to zero past the two maxima on either side (see Fig. 2). For x close to x_n and far from a_n and b_n, we can approximate

$$\psi^{\dagger}_{n,1}(x) \approx \begin{cases} 1 - \sqrt{\frac{\Theta}{2\pi|V''(a_n)|}} \frac{e^{-|V''(a_n)|(x-a_n)^2/2\Theta}}{(x-a_n)}, & a_n \ll x < x_n \\ 1 - \sqrt{\frac{\Theta}{2\pi|V''(b_n)|}} \frac{e^{-|V''(b_n)|(x-b_n)^2/2\Theta}}{(b_n-x)}, & x_n < x \ll b_n \end{cases}. \tag{A13}$$

<?vsk 6pt ?>Evaluating the overlap integral between nearest neighbors in this limit we find

$$\int_{A_{n+1}}^{B_n} dx\, \psi^{\dagger}_{n+1,1}(x)\psi_{n,1}(x) \approx \frac{\sqrt{\beta}\Theta e^{-\beta(b_n-x_n)^2}}{\pi|V''(b_n)|(b_n - x_n)}, \tag{A14}$$

<?vsk 6pt ?>where $\beta = |V''(b_n)|V''(x_n)/2\Theta[|V''(b_n)| + V''(x_n)]$. We can also approximate

$$I_n(B_n) \approx \sqrt{\frac{\pi\Theta}{2|V''(b_n)|}} e^{V(b_n)/\Theta}, \tag{A15}$$

$$I_n(A_n) \approx \sqrt{\frac{\pi\Theta}{2|V''(a_n)|}} e^{V(a_n)/\Theta}, \tag{A16}$$

$$D_n(B_n) \approx \frac{\pi\Theta}{\sqrt{V''(x_n)|V''(b_n)|}} e^{[V(b_n)-V(x_n)]/\Theta}, \tag{A17}$$

$$D_n(A_n) \approx \frac{\pi\Theta}{\sqrt{V''(x_n)|V''(a_n)|}} e^{[V(a_n)-V(x_n)]/\Theta}. \tag{A18}$$

We now write

$$\nu_{n,1} \approx r_n^{KL} + r_n^{KR}, \tag{A19}$$

where

$$r_n^{KL} = \frac{\sqrt{V''(x_n)|V''(a_n)|}e^{-[V(a_n)-V(x_n)]/\Theta}}{2\pi\gamma}, \tag{A20}$$

and

$$r_n^{KR} = \frac{\sqrt{V''(x_n)|V''(b_n)|}e^{-[V(b_n)-V(x_n)]/\Theta}}{2\pi\gamma}, \tag{A21}$$

are Kramers' escape rates over the left and right barrier, respectively. In comparison $\nu_{n,2} \sim V''(x_n)/\gamma$ in the same limit. This order of magnitude estimate for $\nu_{n,2}$ is based on assuming a harmonic shaped confining potential and that the finite height of the barriers only weakly perturbs this state. Using $V(x) = -\Delta V \cos[2\pi(x - x_n)/L]/2$, where $\Delta V \sim V(a_n) - V(x_n) \sim V(b_n) - V(x_n)$ and $L \sim b_n - x_n \sim x_n - a_n$ as a proxy for the potential, we determine that

$$\nu_{n,1} \sim (\Delta V/\gamma L^2)e^{-\Delta V/\Theta}, \tag{A22}$$

$$\nu_{n,2} \sim (\Delta V/\gamma L^2), \tag{A23}$$

$$\psi^{\dagger}_{n,1}(x_n) - 1 \sim \sqrt{\Theta/\Delta V}e^{-\Delta V/\Theta}, \tag{A24}$$

$$\frac{d\psi^{\dagger}_{n,1}(x_n)}{dx} \sim \sqrt{\Theta/\Delta V L^2}e^{-\Delta V/\Theta}, \tag{A25}$$

$$M_{n,n\pm1} \sim e^{-\Delta V/\Theta}, \tag{A26}$$

justifying the approximations in Sec. III for deep wells.

APPENDIX B: NUMERICAL COMPARISON BETWEEN THE HOPPING RATES FOR THE REGULAR PERIODIC POTENTIAL AND KRAMERS' ESCAPE RATE

For the regular periodic potential Eq. (51) we have calculated the hopping rates Eqs. (45)–(47). As shown in Fig. 10, the hopping rates are in good agreement with Kramers' escape rate $r_n^{KL} = r_n^{KR}$ of Eqs. (A20) and (A21).

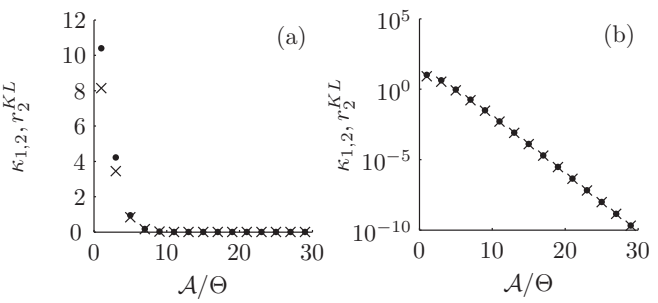

FIG. 10. Hopping rate (crosses) and Kramers' escape rate (dots) of regular system for $\mathcal{A}/\Theta \geqslant 1$ on a linear scale (a) and on a logarithmic scale (b).

[1] F. Baras, M. M. Mansour, and A. L. Garcia, Am. J. Phys. **64**, 1488 (1996).
[2] J. D. Jackson, *Classical Electrodynamics*, 2nd ed. (Wiley, New York, 1975).
[3] W. B. Li, K. J. Zhang, J. V. Sengers, and R. W. Gammom, J. Chem. Phys. **112**, 9139 (2000).
[4] F. Ritort, in *Advances in Chemical Physics*, edited by S. A. Rice (John Wiley and Sons, Hoboken, 2007), Vol. 137.
[5] T. W. Allen and S. H. Chung, Biochim. Biophys. Acta, Biomembr. **1515**, 83 (2001).
[6] E. Abad, J. Reingruber, and M. S. P. Sansom, J. Chem. Phys. **130**, 085101 (2009).
[7] D. Sigg, J. Gen. Physiol. **144**, 7 (2014).
[8] H. Risken, *The Fokker-Planck Equation: Methods of Solution and Applications*, 2nd ed. (Springer-Verlag, Berlin, 1989).
[9] P. Reimann, Phys. Rep. **361**, 57 (2002).
[10] D. Chowdhury, Phys. Rep. **529**, 1 (2013).
[11] C. Bustamante, D. Keller, and G. Oster, Acc. Chem. Res. **34**, 412 (2001).
[12] Z. Koza, J. Phys. A **32**, 7637 (1999).
[13] Y. R. Chemla, J. R. Moffitt, and C. Bustamante, J. Phys. Chem. B **112**, 6025 (2008).
[14] A. Valleriani, S. Liepelt, and R. Liposwky, Europhys. Lett. **82**, 28011 (2008).
[15] V. Bierbaum and R. Lipowsky, PLoS ONE **8**, e55366 (2013).
[16] M. Linden and M. Wallin, Biophys. J. **92**, 3804 (2007).
[17] D. Tsygankov, M. Linden, and M. E. Fisher, Phys. Rev. E **75**, 021909 (2007).
[18] R. Lipowsky, Phys. Rev. Lett. **85**, 4401 (2000).
[19] P. Gaspard and E. Gerritsma, J. Theor. Biol. **247**, 672 (2007).
[20] E. Gerritsma and P. Gaspard, Biophys. Rev. Lett. **5**, 163 (2010).
[21] K. J. Challis and M. W. Jack, Phys. Rev. E **88**, 042114 (2013).
[22] D. Keller and C. Bustamante, Biophys. J. **78**, 541 (2000).
[23] R. Ferrando, R. Spadacini, and G. E. Tommei, Phys. Rev. E **48**, 2437 (1993).
[24] G. Caratti, R. Ferrando, R. Spadacini, and G. E. Tommei, Chem. Phys. **235**, 157 (1998).
[25] P. Jung and B. J. Berne, in *New Trends in Kramers' Reaction Rate Theory*, edited by P. Talkner and P. Hänggi (Kluwer Academic, Netherlands, 1995), p. 67.
[26] G. Lattanzi and A. Maritan, Phys. Rev. E **64**, 061905 (2001).
[27] H. Wang, C. S. Peskin, and T. C. Elston, J. Theor. Biol. **8221**, 491 (2003).
[28] J. Xing, H. Wang, and G. Oster, Biophys. J. **89**, 1551 (2005).
[29] P. Talkner and J. Luczka, Phys. Rev. E **69**, 046109 (2004).
[30] P. Talkner and J. Luczka, Acta Phys. Pol. B **36**, 1837 (2005).
[31] C. Kittel, *Introduction to Solid State Physics* (Wiley, New York, 2004).
[32] G. H. Wannier, Phys. Rev. **52**, 191 (1937).
[33] W. Kohn, Phys. Rev. **115**, 809 (1959).
[34] M. R. Geller and W. Kohn, Phys. Rev. B **48**, 14085 (1993).
[35] F. B. Pedersen, G. T. Einevoll, and P. C. Hemmer, Phys. Rev. B **44**, 5470 (1991).
[36] N. Marzari, A. A. Mostofi, J. R. Yates, I. Souza, and D. Vanderbilt, Rev. Mod. Phys. **84**, 1419 (2012).
[37] J. Singleton, *Band Theory and Electronic Properties of Solids*, 1st ed. (Oxford University Press, Oxford, 2001).
[38] K. J. Challis and M. W. Jack, Phys. Rev. E **87**, 052102 (2013).
[39] P. T. T. Nguyen, K. J. Challis, and M. W. Jack, Phys. Rev. E **93**, 022124 (2016).
[40] J. W. Demmel, *Applied Numerical Linear Algebra*, 1st ed. (SIAM, Philadelphia, 1997).